**Coupled Systems Mechanics,** *Vol. 8, No. 6 (2019) 473-488*
DOI: https://doi.org/10.12989/csm.2019.8.6.473 

# Effects of the geometrical parameters of the core on the mechanical behavior of sandwich honeycomb panel

Settet T. Ahmed*, Salah Aguib[a], Djedid Toufik, Chikh Noureddine and Chellil Ahmed

*Dynamic Motors and Vibroacoustic Laboratory, M'Hamed Bougara University of Boumerdes, Algeria*

*(Received March 8, 2019, Revised July 29, 2019, Accepted October 24, 2019)*

**Abstract.** The present work is the study of mechanical behavior due to variation of the geometrical parameters in the core of the sandwich honeycomb panel. This study has allowed us to increase or decrease the strains and stresses of the panel, in changing the angle of alveolus, as explained and described below. In taking into consideration the results obtained previously to improve the mechanical properties and increase the adhesion of different parts of the panel, without changing the adhesive, we have conceived two new models, in increasing the contact surfaces in boundary of each part of the panel and giving a conical hexagonal shape in his corp.

**Keywords**: honeycomb structure; finite element simulation; delamination; conical hexagonal shape

## 1. Introduction

Several studies were conducted on composite honeycomb sandwich panel in order to improve their mechanical characteristics. This study goes in as part of a previous work (Settet *et al*. (2014)), which has enabled us to identify and locate the critical zones of the sandwich honeycomb panels and highlight them; in this step of work, on one hand we will try to reduce these failures by changing the geometrical parameters without changing the composition materials used in different parts of the panel, in order to change their mechanical characteristics, and another hand we designed two new models of panel. The design is increasing the adhesion surfaces (of contacts) in the aim to reduce delamination, which occurs at the interfaces between different components of the panel, particularly between skins and the core. (Palei and Trepelkova 1965) studied the effect of the shape, size of the cell and the panel thickness on the strength of honeycomb materials, where three types (shapes) of core cells are investigated: regular (symmetric) hexahedral; hexahedral offset by one-half pitch and reinforced hexahedral. This study showed that cores with reinforced cells obey all the laws characteristic of other cores. Proper design requires an understanding of the response of the materials to stress; and, in real engineering design; the stress state is often a complex one. (L.J. Gibson *et al*. 1989) have modeled the elastic buckling, plastic yield and brittle fracture of cellular solids under multi-axial stresses to develop equations describing their failure

*Corresponding author, Ph.D., E-mail: a.settet@univ-boumerdes.dz
[a]Associate Professor, E-mail: s.aguib@univ-boumerdes.dz


http://www.techno-press.org/?journal=csm&subpage=8 ISSN: 2234-2184 (Print), 2234-2192 (Online)

surfaces. Materials with a cellular structure are increasingly used in engineering. Proper design requires an understanding of the response of the materials to stress; and, in real engineering design; the stress state is often a complex one. In this paper we model the elastic buckling, plastic yield and brittle fracture of cellular solids under multi-axial stresses to develop equations describing their failure surfaces. The models are compared to data in the following, companion, paper. (Erik C. Mellquist and Anthony M. Waas 2004) studied the effect of cell size on the out of plane compressive crushing response of circular cell polycarbonate honeycomb (ranging in size from 1 to 14 cells). (Li *et al*. 2014) have been studied the optimizing crashworthiness design of square honeycomb structure; the results obtained show that the square honeycomb exhibits good energy absorption performance in some cases. In the work (Barbarosie and Toader 2010), they had deduced formulae for the shape and topological derivatives for elliptic problems in unbounded domains subject to periodicity conditions. The second part of this work was devoted to implementation of an optimization algorithm for periodic problems which alternates shape and topology optimization; where the numerical method was tested for the design of periodic microstructures (Barbarosie and Toader 2010). (Ju *et al*.2012) have explored a flexible structural application of honeycombs in shear. While pursuing a hexagonal honeycomb structure with in-plane shear properties similar to an elastomer, they investigated the effect of various geometric parameters on the in-plane effective elastic properties (Young's and shear moduli) of conventional and auxetic hexagonal honeycombs with mild-steel and polycarbonate. (Barbarosie 2003) described a numerical approach to the optimization of effective properties of periodic perforations in an infinite body, in the frameworks of heat conduction and of linear elasticity. He implemented a special finite element mesh in order to deal with the periodic nature of the problem. (Tounsi*et al*. 2015) have investigated experimentally the dynamic behavior of an aluminum alloy honeycomb under mixed shear-compression loading with a special attention on the combined effects between the cells in-plane orientation and the loading angles. (Paz *et al*. 2015) proposes in their research a new design of an aircraft's vertical strut. The design consists of hollowed aluminum square tube with a glass-fiber reinforced polymer honeycomb-shaped inner structure. Size and shape surrogate-based optimization techniques are used, with the thicknesses of both materials, cell size and cell shape as design variables. The objective function chosen for the single-objective optimization is the specific energy absorption, while the metrics for the multi-objective optimization are the peak force, mass, absorbed energy and the specific energy absorption. An improvement of 22% of the specific energy absorption with low peak force values is obtained from the single-objective optimization by significantly changing all design variables. When compared to the baseline model, the optimized models show substantial improvement, increasing the specific energy absorption by 65% or reducing the peak force by over 55%. It has been observed an important effect of the cell shape on the model's performance. (Sardar *et al*. 2015), investigated the elastic behavior of periodic hexagonal honeycombs over a wide range of relative densities and cell geometries, using both theoretical study and numerical approaches. Previous modeling approaches are reviewed and their limitations identified. (Correa *et al*. 2015) investigates honeycomb structures whose unit cells are created from curved beam structures that are designed to provide negative stiffness behavior and a single stable position. Several studies have been paid to the removal of structural defects. (Cui *et al*. 2019) have studied; the branch point algorithm was first constructed for the determination of the structural irregularity of the honeycomb structure, in order to identify the geometric defect of similar cellular structures. Equivalent sandwich panels composed of auxetic and conventional honeycomb cores and metal facets are analyzed and compared for their resistance performances against impulsive loadings. The dynamic behaviors of

these structures are numerically investigated, taking into account the rate-dependent effects. The Johnson-Cook model is employed to describe the dynamic responses of the composite sandwiches subjected to high strain-rate loadings (Imbalzano *et al*. 2018). For multifunctional optimization design of honeycomb structures, the high stiffness hierarchical honeycombs with stochastic Voronoi substructures (HHSVS) are proposed by substituting cell walls of the regular hexagonal honeycombs (ORHH) with Voronoi honeycomb lattices of equal mass (Wang *et al*. 2019).

In this work, a theoretical study of the mechanical behavior of three-point flexural sandwich beams with a numerical simulation under the Ansys software was made to show the influence of cell orientation angles on the mechanical behavior of the panels.

## 2. Theoretical study

### *2.1 Geometry and displacement*

The honeycomb panel (sandwich panel) is comprised by a three parts: the core, upper and lower skins, as shown in Fig. 1. The geometrical and mechanical properties of a skin, adhesive and honeycomb core of this honeycomb panel are shown in Fig. 2 and described in Table 1 and Table 2.

The shear effect is very important for the behavior of sandwich panels and this part is to explain as clearly as possible what it is. When a load directed towards the positive "z" is applied to the right end of the beam, it induces a bending and shearing moment and deforms upwards along a certain curve (see Fig. 3). Expression of the transverse shear is given by equation 1.It is important to understand that the angle $\beta$ is the angle of the section caused by the bending moment only, regardless if the shear is taken into account or not. $\beta$ is subsequently called bending angle. The derivative of the transverse displacement of the neutral fiber represents the slope of the neutral fiber and $\gamma$ is the angle of the section due to shear only. A more intuitive way to understand this relationship is to express the previous equation as follows

$$\frac{\partial w}{\partial x} = \gamma - \beta \tag{1}$$

This equation reflects the fact that the slope of the neutral plane is a function of the two angles $\beta$and $\gamma$measured from the horizontal.The shear on an infinitesimal element of a beam whose right end is shear loaded, is shown in Fig. 3.

In our work, we have adopted Timoshenko's theory; the latter is of course more representative of reality since it takes into account the effect of bending and shear deformations simultaneously.

### *2.2 Behavior of sandwich in flexion*

#### *2.2.1Three-point bending*

Fig. 4 represents a honeycomb sandwich beam subjected to three-point bending

##### *2.2.1.1 Normal stress*

In the case of a central loading of the beam (Fig.4), the bending moment is written

$$M = \frac{q}{2}x \qquad \text{for} \qquad 0 \leq x \leq L/2 \tag{2}$$


Fig. 1 Component of honeycomb panel

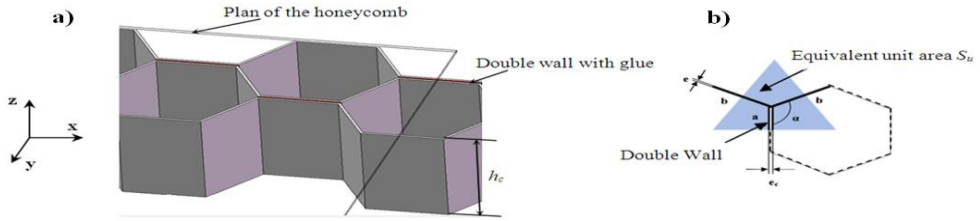


Fig. 2 (a) Reference associated with the honeycomb and (b) geometry of an elementary cell

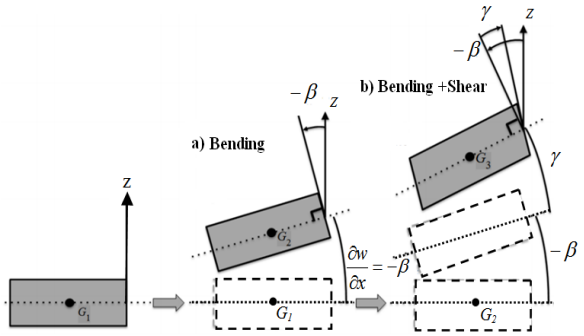


Fig. 3 Bending and shear deformation representation

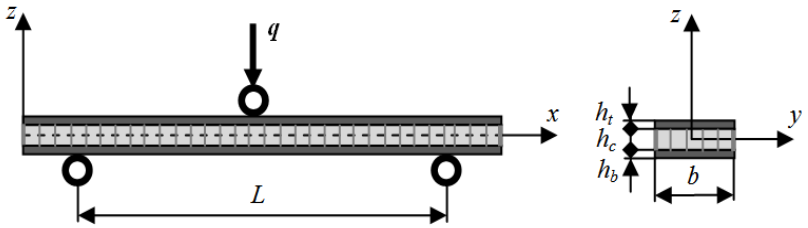


Fig. 4 Three-point bending

$$M = \frac{q(L-x)}{2} \quad \text{for} \quad L/2 \le x \le L \tag{3}$$

$q$ is the applied load and x the distance from the origin.
The tensile or compressive stresses in the skins are then

$$\sigma_t = \frac{M}{D} E_t \quad \text{for} \quad -\frac{h}{2} \le z \le -\frac{h_c}{2} \quad \text{and} \quad \frac{h_c}{2} \le z \le \frac{h}{2} \tag{4}$$

where D is the bending stiffness given by the following relation (DIAB sandwich handbook)

$$D = \int Ebz^2\,dz = \frac{E_t b h_t^3}{6} + 2E_t b h_t \left(\frac{h}{2}\right)^2 + \frac{E_c b h_c^3}{12} = \frac{E_t b h_t^3}{6} + \frac{E_t h_t b h^2}{2} + \frac{E_c b h_c^3}{12} = 2D_t + D_0 + D_c \quad (5)$$

$h_{t,b}$ and $E_{t,b}$are respectively the thickness and elasticity modulus of the skin material (identical skins).

$h_c$ and $E_c$are respectively the thickness and elasticity modulus of the core material.

$2D_{t,b}$: stiffness of the skins with respect to their own neutral axis.

$D_0$: contribution to the stiffness bending of the skins with respect to the neutral axis of the sandwich at the center of the core for a symmetrical sandwich.

$D_c$: stiffness provided by the core relative to its neutral axis

The maximum is obtained for $\pm\frac{h}{2}$ and $x = \frac{L}{2}$

$$\sigma_{t\,max} = \pm\frac{qLh}{8D}E_t \quad (6)$$

For the core, we have

$$\sigma_c = \pm\frac{Mz}{D}E_c \text{for} -\frac{h_c}{2} \le z \le -\frac{h_c}{2} \quad (7)$$

The maximal plane stresses supported by the core are then expressed by

$$\sigma_{c\,max} = \frac{qLt_c}{8D}E_c \quad (8)$$

### *2.2.1.2 Shear stress*

With regard to the shear stress in the core, due to the heterogeneity of the structure, considering the elastic modulus change in the transverse direction, from where

$$\tau_c = \frac{T}{A} \quad (9)$$

where *A* is the shear section.

The distribution of the shear stresses is illustrated in Fig. 5, (Engin, M. R.).

In the case of a central load of a beam (Fig.4), the shear force is written:

$$T = \frac{q}{2} \quad \text{for} \quad 0 \le x \le L/2 \quad (10)$$

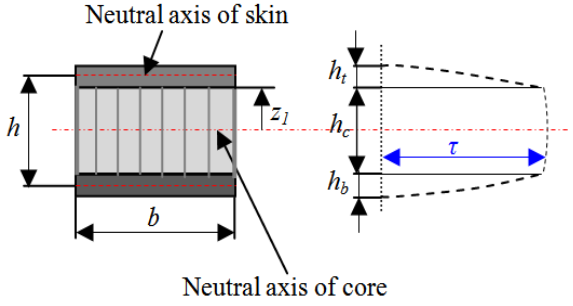


Fig. 5 Distribution of shear stresses

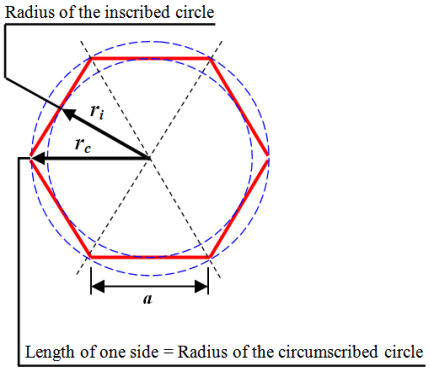


Fig. 6 Geometric characteristics of a cell

$$T = -\frac{q}{2} \text{ for } \quad L/2 \leq x \leq L \tag{11}$$

Therefore shear stress is given by

$$\tau_c = \frac{q}{2A} \tag{12}$$

For *n* viols, the shear stress is written as follows

$$\tau_c = \frac{q}{2nA} \tag{13}$$

The geometric characteristics of a cell are given in Fig. 6.
where: $a$ is the length of one side, $r_c$ is the radius of the circumscribed circle and $r_i$ is the radius of the inscribed circle.

The section of a regular hexagon side *A* is

$$A = \frac{3\sqrt{3}}{2} a^2 \tag{14}$$

Finally, the three-point bending shear stress is given as follows

$$\tau_{c\,max} = \frac{q}{3n\sqrt{3}a^2} \tag{15}$$

The surface of contact between the core and the skin in the case of panels: NHP-O, NHP-X and the others are respectively: $A_{NHP\text{-}O}$ = 303.27 mm$^2$, $A_{NHP\text{-}X}$= 378.42 mm$^2$, $A_{others}$= 99.83 mm$^2$.

## 3. Numerical simulation

The system of coordinates is chosen so that the plane (x, y) is the middle plane, and to determine the strains and stresses, we must take inconsideration the hypothesis of the theory of sandwich (Jean-Marie Berthelot):

1. For thin laminated plates, the total laminate thickness $h$ is usually small compared to other plate dimensions (the thickness of the core is much higher than that of the skins: $h \gg h_1, h_2$).

2. The displacements of the core $u_a$ and $v_a$ in the directions x and y are the linear functions of the coordinate *z*.

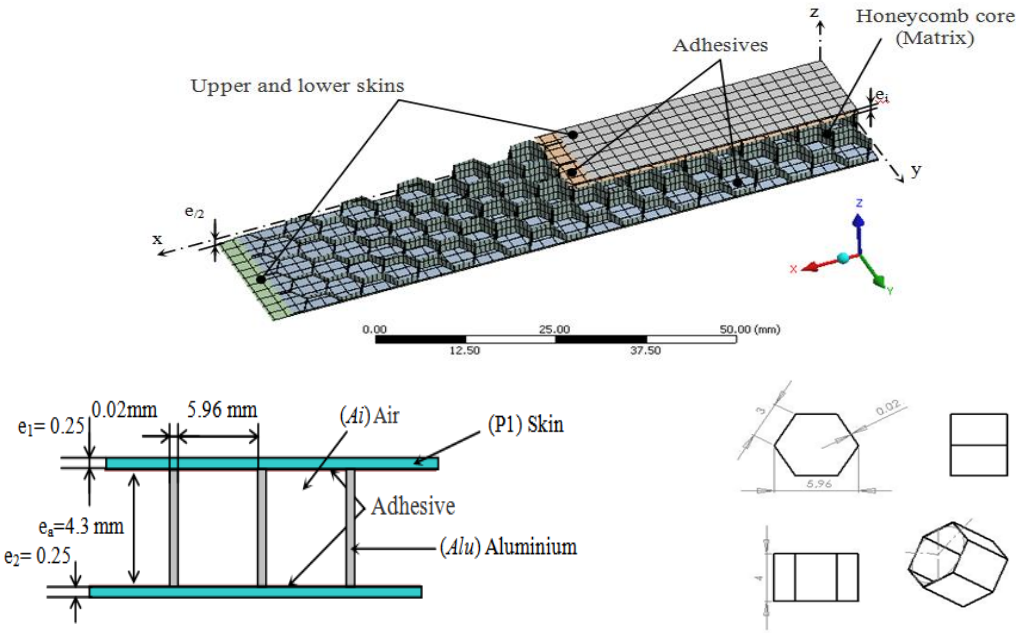


Fig. 6 Geometric characteristics of a cell

Table 1 Mesh characteristics

| Denomination | Nodes | Elements |
|---|---|---|
| Skins | 4322 | 572 |
| Adhesives | 4322 | 572 |
| Honeycomb core | 32176 | 4092 |
| Total | 49464 | 6380 |
| Total elements of contact | 10032 | |

3. The displacements $u$ and $v$ in the directions x and y are uniform in the thickness of the skins.
4. The transverse displacement $w$ was independent of the variable z, the strain $\varepsilon_{zz}$ are neglected.
5. The core transmits only transversal shear stresses: the stresses $\sigma_{xx}, \sigma_{yy}, \sigma_{xy}$ and $\sigma_{zz}$ are neglected.
6. Transverse shears stresses $\sigma_{xz}$ and $\sigma_{yz}$ are neglected in the skins.

Finally, the theory deals with the problems of elasticity of small deformations.

### *3.1 Implementation*

Sandwich structures are constituted by an aluminum honeycomb core and a skin made of different materials. For the numerical solution problem, it was necessary to follow a specific process in order to achieve coherent results.

Simulations were performed on the Ansys software. The mesh model takes into account the entire structure that has been meshed with a three-dimensional quadratic hexahedral structured

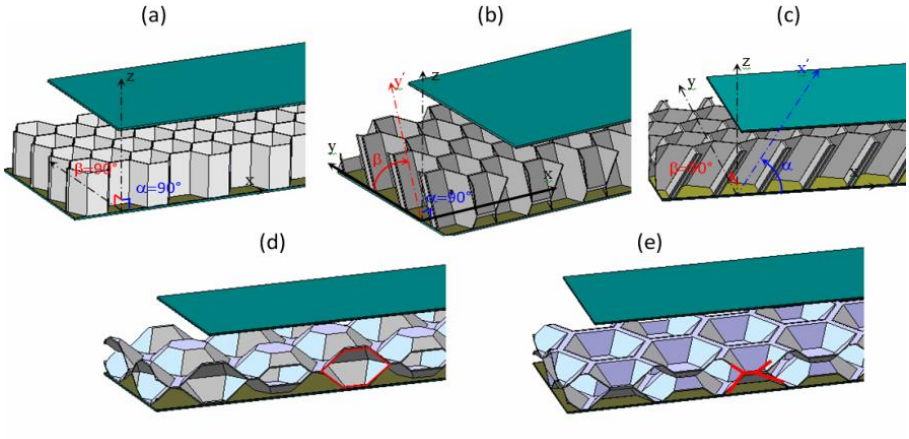


Fig. 8 Geometry and design of the honeycomb sandwich panels: (a) Honeycomb panel β= 90°; $\alpha$ =90°, (b) β, α=90°, (c)β= 90°/ $\alpha$=, (d) New honeycomb panel in O shape (NHP-O-) (e) New honeycomb panel in X shape (NHP-X-) where: NHP-O-: New honeycomb panel in O shape, and NHP-X- : New honeycomb panel in X shape

Table 2 Different geometric configurations of the panels

| | Panels | | | | | | | | | | | |
|---|---|---|---|---|---|---|---|---|---|---|---|---|
| | 1 | 2 | 3 | 4 | 5 | 6 | 7 | 8 | 9 | 10 | 11 | 12 |
| $\alpha$ | 90° | | | | 30 | 45° | 60° | 120° | 135°° | 150° | NHP-O- | NHP-X- |
| $\beta$ | 30° | 45° | 60° | 90° | | | | | | | | |

element (H20) with 20 nodes. For this model, the mesh chosen makes it possible not to weigh down the computation while keeping a good precision with the results. Excessive refinement does not give better results therefore the mesh presented in Fig. 7 is relatively good, it has 6380 elements and 49464 nodes. The mesh results are given by Table 1.

### *3.2 Geometry and design of the honeycomb sandwich panels*

To study the core's geometrical variation of the sandwich honeycomb panels, twelve cases (specimens) with different cores discussed above are summarized as following:

The cells have two angles $\alpha$ and $\beta$ equal to 90°. i.e., they are placed perpendicularly to the skin (conventional standard) (Fig. 8(a)); thereafter we be making oblique cells (transversally) $\alpha$=90° and varying $\beta$ to 30°,45°and 60° respectively (Fig. 8(b)); then we be making oblique cells longitudinally $\beta$=90° and varying $\alpha$ to 30°,45°and 60°, also (longitudinally) varying $\alpha$ to 120°,135°and 150° respectively (Fig. 8(c)), where we increased the adhesion surface of the core, of which the first is O-shaped (Fig. 8(d)) and the second X-shaped (Fig. 8(e)) we used, simultaneously, two types of material for all of the panel's skins; the first one is made with aluminum , the second is made with glass epoxy.

The Table 2 above represents the geometric characteristics of the core of the studied panels.
In three points bending, the panels 5, 6 and 7 have the same geometry with 10, 9 and 8 respectively, which gives the same result. This is enough to study one case.

Table 3 Mechanical properties of a skin, adhesive and honeycomb core

| | Skins | | Adhesive | Core |
|---|---|---|---|---|
| Materials | Aluminum | Glass epoxy | Structure adhesive | Aluminum |
| Young modulus [MPa] | 71000 | 54000 | 1,7 10-3 | 71000 |
| Poisson's ratio | 0,33 | 0,25 | 0,245 | 0,33 |
| Density [kg/m$^3$] | 2770 | 950 | 950 | 2770 |
| Tensile yield strength [MPa] | 280 | 1035 | 14 | 280 |
| Tensile ultimate strength [MPa] | 310 | 28 | 31 | 310 |

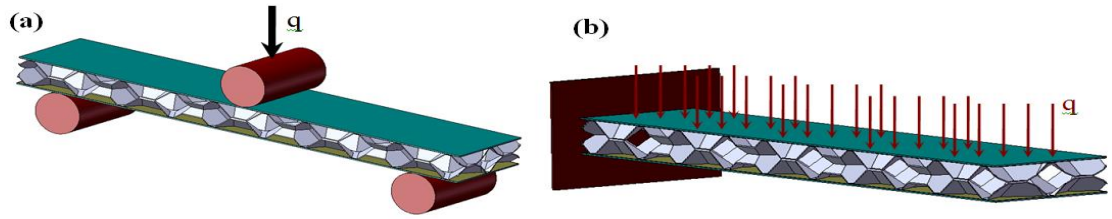


Fig. 9 Honeycomb panel under load (a)Honeycomb panel in three-point bending and (b) Cantilever honeycomb panel with uniform load

### *3.3 Materials and mechanical properties*

The analyses were carried out using a three-point bending in the first case and clamped bending in the second case. The skins of the sandwich panels used in this study are made of glass epoxy in the first time and aluminum skins in the second time. The sandwich panels have the mechanical properties of the basic materials which are given in Table 3.

In this study, we will present the result of honeycomb panel in three-point bending and in cantilever with uniform load; the load (21N) applied linearly in the first case and distributed uniformly on surface in the second. The surrounding temperature is 20℃. Fig. 9(a) and 9(b).

## 4. Result and discussion

The figures below represent different results of the twelve models of honeycomb panels with glass-epoxy or aluminum skins.

### *4.1 Displacement of honeycomb panels*

The figure (Fig. 10), and (Fig. 11) represent respectively the curves of displacement of honeycomb panels versus geometric variation of the core's sandwich honeycomb panels in z direction in three-point bending and cantilever with uniform load; we notice that the better result obtained of the maximum displacement of honeycomb panels with in glass epoxy or aluminum skin is the new honeycomb panel in x shape (panel eleven), that represent in the first case (Fig.10) respectively 4.3899 $10^{-2}$ mm and 3.5479 $10^{-2}$ mm and in the second case (Fig.8) respectively 3,3972 $10^{-01}$ mm and 2,7452 $10^{-01}$ mm, where that's the minimum displacement.

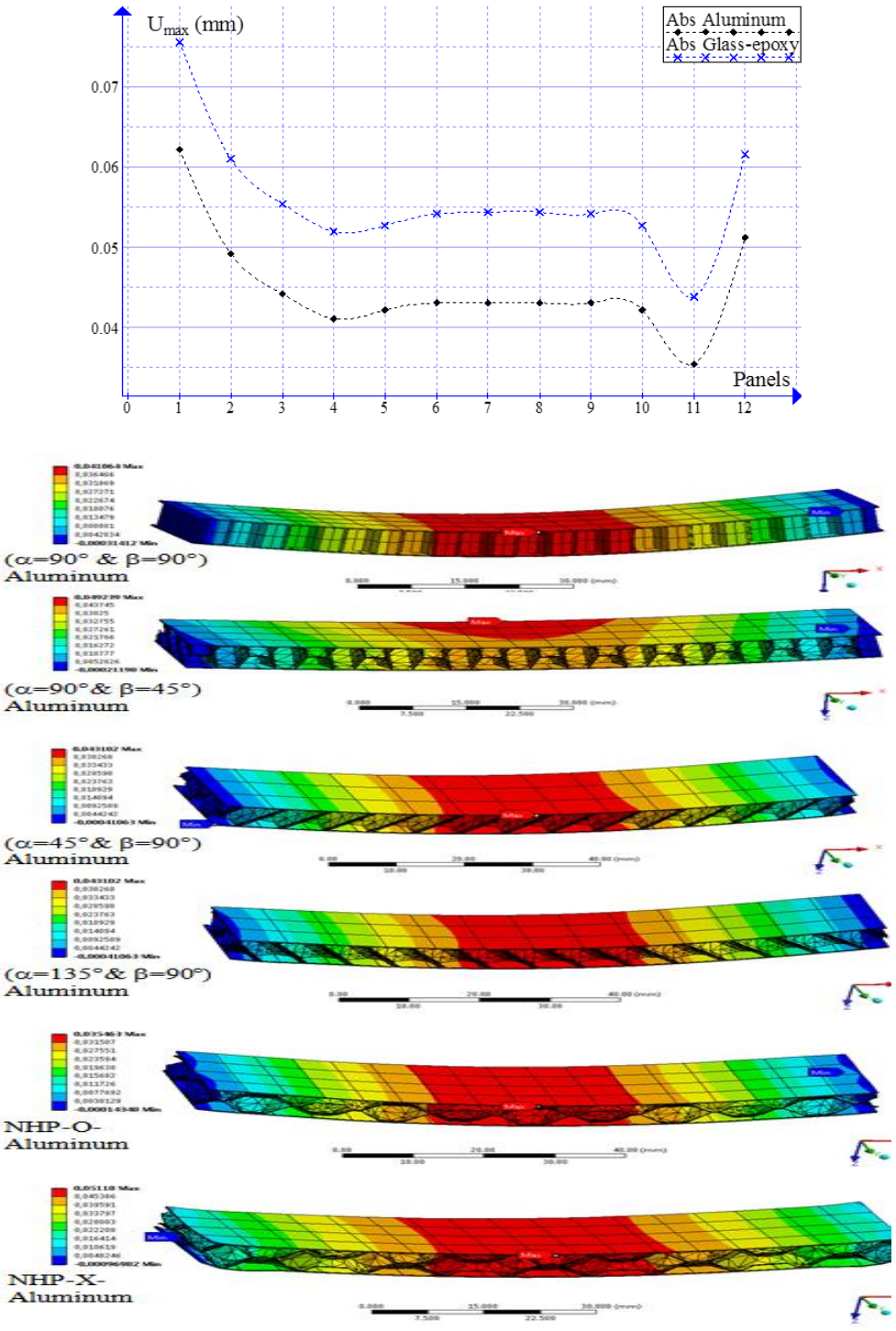


Fig. 10 Displacement of honeycomb panels with glass-epoxy or aluminum skins in z direction in three-point bending

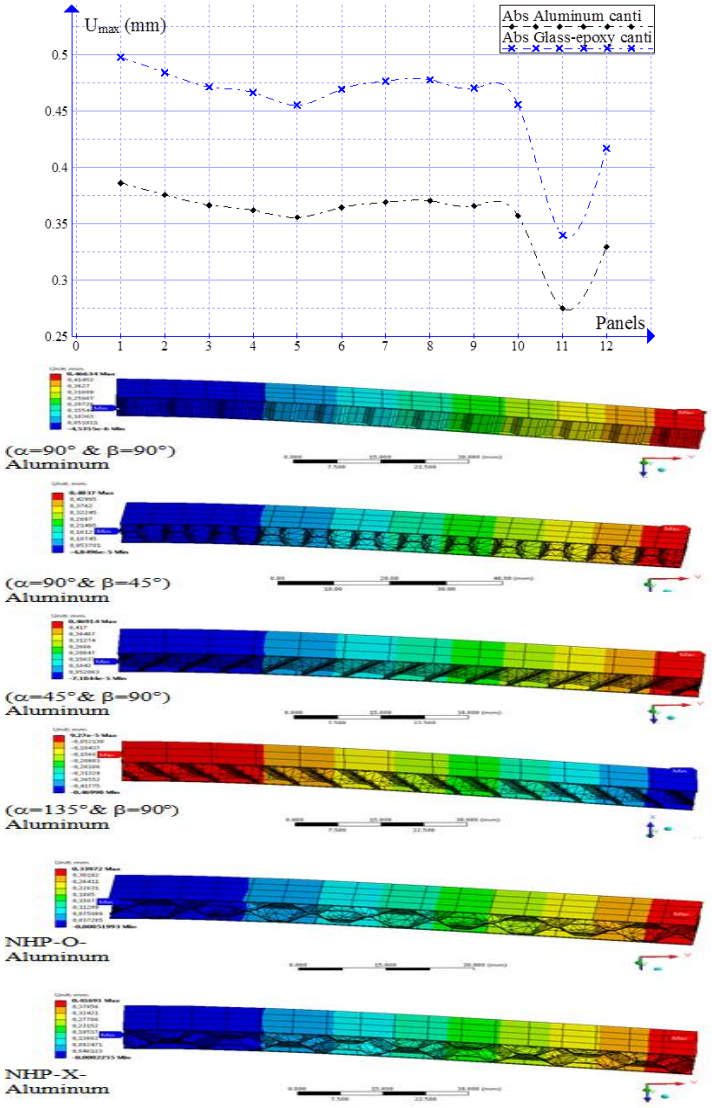


Fig. 11 Displacement of honeycomb panels with glass-epoxy or aluminum skins in z direction in cantilever with uniform load

### *4.2 Maximum principal stress*

Fig. 12 represents a maximum principal stress in absolute value of the panels with glass-epoxy or aluminum skins in three-point bending **(**Fig. 12(a)**)** and cantilever with uniform load **(**Fig. 12(b)**)**. In the first case **(**Fig. 12(a)**)** the fourth, seventh and eighth panel of glass epoxy skin and aluminum skin, the stress doesn't exceed the value of10,457 MPa, thus, it is considered as the smallest stress in comparison with all the other panels, otherwise, the most important stress is of the second panel. A small difference is remarkable between the panels of glass epoxy's skin and the aluminum one. In the second case **(**Fig. 12(b)**),** the fourth panel of glass epoxy skin and the

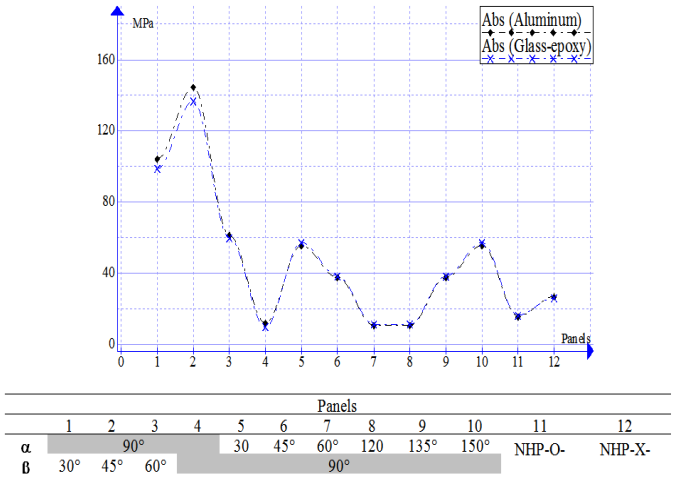


(a)

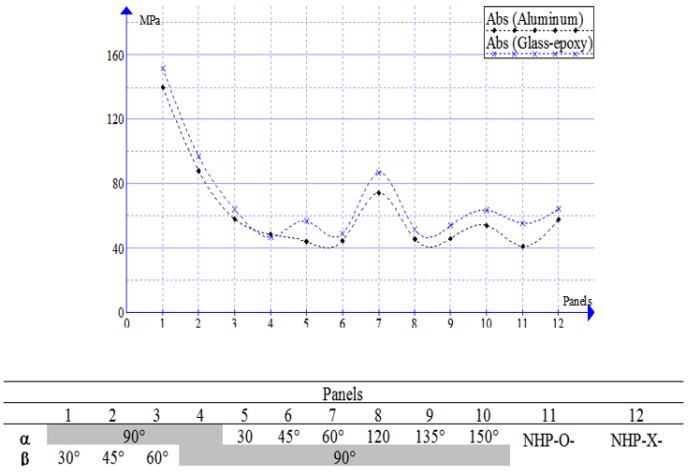


(b)

Fig. 12 Maximum principal stress of panel with glass-epoxy and aluminum skins (a) three-point bending and (b) cantilever with uniform load

eleventh panel of aluminums kin, have respectively 4,6954 $10^1$MPa and 4,12915 $10^1$MPa of stress, thus, it is considered as the smallest stress in comparison with all the other panels, otherwise, the most important (high) principal stress is of the first panel. The panels: 5, 6, 8 and 9 take a little variation relatively with the fourth panel (conventional standard). A small difference is remarkable between the panels of glass epoxy's skin and the aluminum one.

### *4.3 Maximum shear elastic strain*

The figure (Fig.13) represent maximum shear elastic strain of panel with glass-epoxy or aluminum skins (Fig.13(a)) three-point bending and (Fig. 13(b)) cantilever with uniform load. We noted that strain doesn't exceed the value of 0.17 % in the panel in glass epoxy skin and in the panel in aluminum skin, in other part we can observe from third panel until eleventh shear doesn't

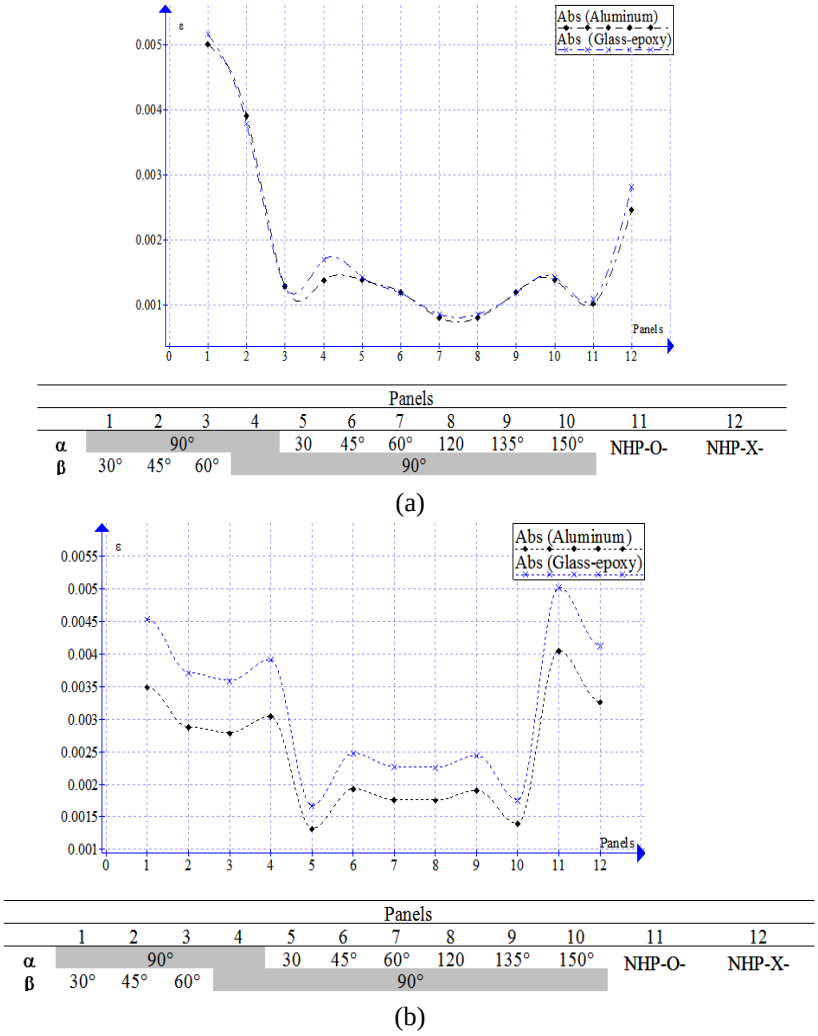


Fig. 13 Maximum shear elastic strain of panel with glass-epoxy and aluminium skins (a) three-point bending and (b) cantilever with uniform load

very significant (Fig. 13(a)), the maximum shear elastic strain in cantilever with uniform load (Fig. 13(a)) of panel with glass-epoxy or aluminum skins from fifth up to tenth specimen is less than other panels and it doesn't exceed 0.25%.

### *4.4 Maximum shear stress*

Fig. 14 represent maximum shear stress of panel with glass-epoxy or aluminum skins (Fig. 14(a)) three-point bending and (Fig. 14(b)) cantilever with uniform load. We noted that the maximum shear doesn't exceed the value of 44.571 MPa in the panel with glass epoxy skin or in the panel in aluminum skin, moreover from third panel to eleventh shear is not very significant (Fig. 14(a)). The maximum shear elastic stress of panel with glass-epoxy or aluminum skins in cantilever with uniform load (Fig.14(a)) doesn't exceed 36MPa from third to twelfth specimen.

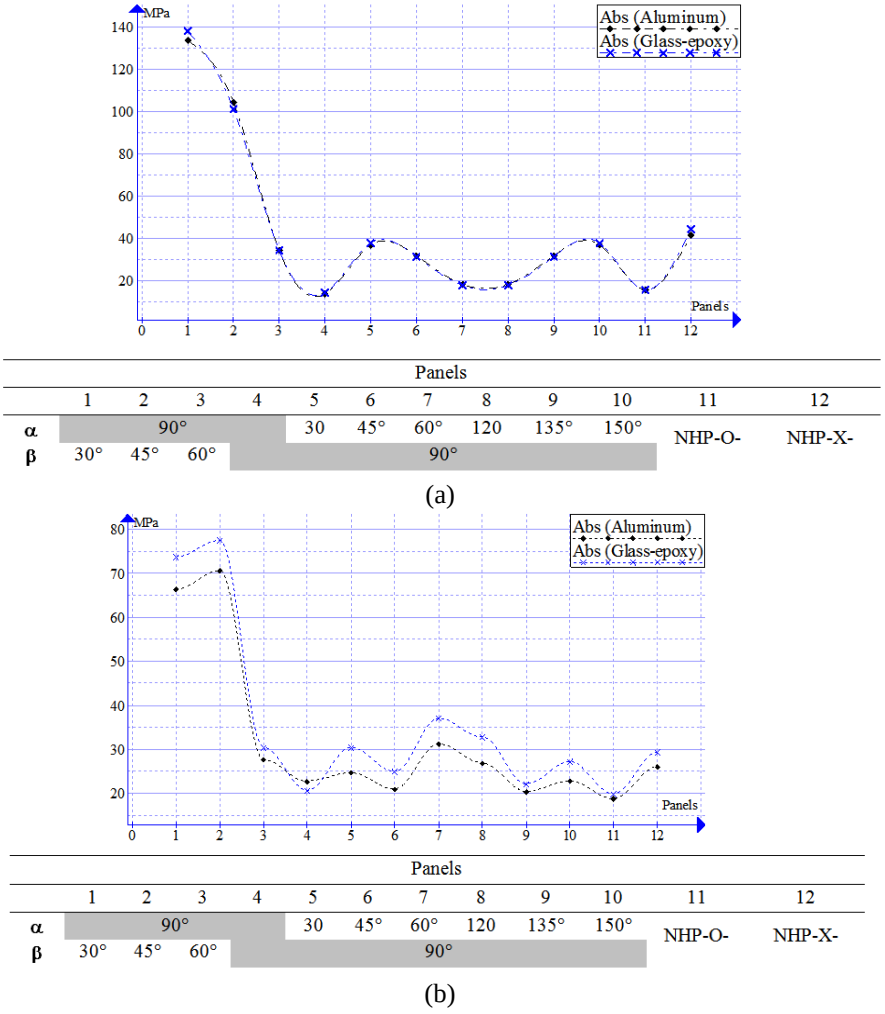


Fig. 14 Maximum shear stress of panel with glass-epoxy or aluminium skins three-point bending and (b) cantilever with uniform load

We can add in, in three-point bending, the displacement in the new specimen (11) is reduced up to 77% and increasing up to 147% (new specimen (01)), and in cantilever, it is reduced up to 144% (Fig.12) (new specimen (11)) compared conventional panel(specimen (04)). In all cases, the maximum shear elastic strains do not exceed 0.52 % (Fig.13), which is considered very small. On the other part, the minimum value of maximum shear stress of panel with glass-epoxy or aluminium skins is observed in the case fourth 4 and eleventh 11 panels. This result is due to the surface increasing, and concentration of each stress are distributed on the hexagonal surface, thereafter, this last are redistributed on the intermediate surfaces, this reduces the forces on each cell (4).

### *4.5 Synthesis of results*

A kind of innovative honeycomb panel with variable geometry was investigated here for its

bending behavior by using finite element model implemented in Ansys software. In this study, series of numerical simulations of three-point bending were carried out for the new honeycomb sandwich with variable geometry. The numerical results found confirm that the geometric shape largely enhances the stiffness of the structure, which contributes a lot to the improvement of the bending resistance capacity. It was found that the bending performance heavily relay on the geometric configuration of the honeycomb cells. In addition, the sandwich panel where the honeycomb core having a large contact area also shows better mechanical behavior in the simulation. All these achievements provide more likelihood of designing composited high-performance sandwich.

## 5. Conclusions

This work allowed us to appreciate behaviour of new specimen of panel conceived (Four new concepts were adopted) and conventional panel, in three-point bending and cantilever with uniform load with glass-epoxy and aluminium skins, where:

- The displacement of specimen (11) in z direction was the smallest one,
- The maximum principal stress is reduced in the case of panels (8) and (11),
- The maximum shear elastic strain was obtained in the case of panels from 1 to 4 and also from 11to 12,
- The minimum value of maximum shear stress was obtained in the case of panels4 and 11.

The core transmits only transversal shear, stresses $\sigma_{xx}$ , $\sigma_{yy}$, $\sigma_{xy}$ and $\sigma_{zz}$ are neglected.

If shear increase, strain decrease and inversely. This result is due of surface contact between core and skins (top and bottom). If we increase contact surface, shear increase and strain decrease and inversely.

If we change alveoli angle(shape of honeycomb core), the quadratic moment of alveoli change and strength of panel change, which affect overall strength panel. There is a high resistance in the case of the panel 4, where $\alpha = \beta = 90°$, on the other hand we observe a smaller resistance in the case of panel 1, where $\alpha = 90°$, $\beta = 30°$.

This study has shown that, despite the difficulties posed by honeycomb sandwich panels, we can determine their behavior for the three-point bending using numerical modeling under the Ansys software and we can conclude that the results deduced from this simulation are very satisfactory.

## Acknowledgments

I thank you my colleagues researcher of the mechanical Dynamic Motors and Vibroacoustic Laboratory, M'Hamed Bougara University of Boumerdes, Algeria for their help.

## References

Barbarosie, C. (2003), "Shape optimization of periodic structures", *Comput. Mech.*, **30**(3), 235-240. https://doi.org/10.1007/s00466-002-0382-3.

Barbarosie, C. and Toader, A.M. (2010), "Shape and topology optimization for periodic problems Part I: The shape and the topological derivative", *Struct. Multidisciplin. Optim.*, **40**(1), 381-391.

https://doi.org/10.1007/s00158-009-0378-0.
Barbarosie, C. and Toader, A.M. (2010), "Shape and topology optimization for periodic problems Part II: optimization algorithm and numerical examples", *Struct. Multidisciplin. Optim.*, **40**(1), 393-408. https://doi.org/10.1007/s00158-009-0377-1.
Berthelot, J.M. (2012), *Mechanics of Composite Materials and Structures*, 5e Edition: Tec & Doc Lavoisier.
Correa, D.M., Seepersad, C.C. and Haberman, M.R. (2015), "Mechanical design of negative stiffness honeycomb materials", *Integrat. Mater.*, **4**, 1-11. https://doi.org/10.1186/s40192-015-0038-8.
Cui, C., Wang, Z., Zhou, W., Wu, Y. and Wei, W. (2019), "Branch point algorithm for structural irregularity determination of honeycomb", *Compos. Part B*, **162**(1), 323-330. https://doi.org/10.1016/j.compositesb.2018.10.062.
Engin, M. R. (2005), "Characteristics of innovative 3-D FRP sandwich panels", Ph.D Dissertation, North Carolina State University, Raleigh, North Carolina, U.S.A.
Erik, C., Mellquist, A. and Waas, M. (2004), "Size effects in the crushing of honeycomb structures", *Proceedigns of the 45th AIAA/ASME/ASCE/AHS/ASC Structures Structural Dynamics and Materials Conference*, Palm Springs, California, U.S.A., April.
Gibson, L.J., Ashby, M.F., Zhang, J. and Triantafillou T.C. (1989), "Failure surfaces for cellular materials under multiaxial loads—I. Modelling", *Int. J. Mech. Sci.*, **31**(9), 635-663. https://doi.org/10.1016/S0020-7403(89)80001-3.
Imbalzano, G., Linforth, S., Ngo, T.D., Lee, P.V.S. and Tran, P. (2018), "Blast resistance of auxetic and honeycomb sandwich panels: Comparisons and parametric designs", *Compos. Struct.*, **183**, 242-261. https://doi.org/10.1016/j.compstruct.2017.03.018.
Ju, J., Summers, J.D., Ziegert, J. and Fadel, G. (2012), "Design of honeycombs for modulus and yield strain in shear", *J. Eng. Mater. Technol.*, **134**(1), 1-15. https://doi.org/10.1115/1.4004488.
Li, M., Deng, Z.Q., Guo, H.W., Liu, R.Q. and Ding, B.C. (2014) "Optimizing crashworthiness design of square honeycomb structure", *J. Central South Univ.*, **21**(3), 912-919. https://doi.org/10.1007/s11771-014-2018-0.
Palei, M.I. and Trepelkova, L.I. (1965), "Effect of the shape and size of the cell on the compressive strength of honeycomb cores", *Polymer Mech.*, **1**(3), 20-22. https://doi.org/10.1007/BF00858797.
Paul, R.H. and John, K. (2006), "The mechanics of pyramids", *Int. J. Solids Struct.*, **43**(9), 2693-2709.
Paz, J.J., Díaz, J., Romera, L. and Costas, M. (2015), "Size and shape optimization of aluminum tubes with GFRP honeycomb reinforcements for crashworthy aircraft structures", *Compos. Struct.*, **133**, 499-507. https://doi.org/10.1016/j.compstruct.2015.07.077.
Sardar, M. and Lorna, G. (2015), "Effective elastic properties of periodic hexagonal honeycombs", *Mech. Mater.*, **91**, 226-240. https://doi.org/10.1016/j.mechmat.2015.07.008.
Settet, A.T., Nour, A., Zahloul, H. and Naceur, H. (2014), "Evaluation of damage and fracture mechanisms of different characteristic honeycomb structures under thermomechanical loading", *Mech. Compos. Mater.*, **50**(5), 903-922. https://doi.org/10.1007/s11029-014-9452-9.
Tounsi, R., Markiewicz, E., Haugou, G., Chaari, F. and Zouari, B. (2016), "Dynamic behaviour of honeycombs under mixed shear-compression loading: Experiments and analysis of combined effects of loading angle and cells in-plane orientation", *Int. J. Solids Struct.*, **80**, 501-511. https://doi.org/10.1016/j.ijsolstr.2015.10.010.
Wang, B., Ding, Q., Sun, Y., Yu, S., Ren, F., Cao, X. and Du, Y. (2019), "Enhanced tunable fracture properties of the high stiffness hierarchical honeycombs with stochastic Voronoi substructures", *Result. Phys.*, **12**, 1190-1196. https://doi.org/10.1016/j.rinp.2018.12.068.